International Journal of Medical and Pharmaceutical Research

Online ISSN-2958-3683 | Print ISSN-2958-3675
Frequency: Bi-Monthly
Available online on: https://ijmpr.in/

Original Article

Role of Sonoelastography in the Evaluation of Major Salivary Gland Pathologies

Umamaheshwari K B[1], Abhilasha. S[2], Manasa M.R[3], Manupratap N[4]

[1]*Associate professor, Department of Radiodiagnosis, MMCRI, Karnataka, India*
[2]*Junior resident, Department of Radiodiagnosis, MMCRI, Karnataka, India*
[3]*Assistant professor, Department of Radiodiagnosis, MMCRI, Karnataka, India*
[4]*Professor & Head, Department of Radiodiagnosis, MMCRI, Karnataka, India*

OPEN ACCESS

Corresponding Author:

Dr Abhilasha. S
Junior resident, Department of Radiodiagnosis, MMCRI, Karnataka, India

Received: 12-06-2026
Accepted: 15-07-2026
Available online:31-07-2026

ABSTRACT

Background: B-mode ultrasonography is a recommended first-line imaging modality for salivary gland lesions; however, overlapping morphological features may limit differentiation of benign and malignant pathologies. Sonoelastography provides qualitative and quantitative assessment of tissue stiffness and may improve lesion characterization.
Objective: To evaluate the role of sonoelastography in the assessment of major salivary gland pathologies in adults.
Methods: A cross-sectional study was conducted at KR and Cheluvamba Hospitals, Mysore, from August 2024 to March 2026. Fifty patients with major salivary gland pathologies underwent B-mode ultrasonography and sonoelastography using a Mindray DC 80 with an L9-3E linear transducer. Strain ratio and shear-wave elastography (SWE) values were assessed and compared with ultrasound findings.
Results: The mean age of participants was 48.6 years. Sialolithiasis and Stensen's duct stenosis showed the highest elastographic scores (3.7±0.5 and 3.5±0.5, respectively), followed by chronic inflammation (3.2±0.4) and primary Sjögren's syndrome (3.1±0.5), while pleomorphic adenomas had the lowest score (2.8±0.5). Strain ratios were significantly higher in sialolithiasis and duct stenosis ($p<0.001$), with 95.6% diagnostic accuracy at a cutoff of 1.22 (AUC 0.938; 95% CI: 0.825–0.987). SWE values were highest in sialolithiasis (82 kPa) and stenosis (72 kPa), compared with 24 kPa in healthy individuals.
Conclusion: Sonoelastography, strain ratio, and SWE demonstrate potential utility in differentiating major salivary gland pathologies and complement conventional ultrasonography.

Keywords: *Parotid gland; Salivary gland; Sonoelastography; Strain ratio.*

INTRODUCTION

Salivary glands are small structures located in the head and neck, playing a crucial role in overall quality of life. Adequate saliva production helps maintain oral moisture, which is essential for bolus formation, swallowing, dental health, and general well-being. Additionally, aesthetic factors are important, as the parotid glands, found in the preauricular area, contribute to facial contour. Tumors of the salivary glands make up a notable portion of oral and maxillofacial pathological conditions. [1].

Salivary gland diseases vary in severity, from mild inflammatory conditions to a range of benign and malignant tumors. Most of these conditions present as gland enlargement, with the majority of tumors developing in the parotid gland, while 10–15% arise in the submandibular gland. The estimated annual incidence of salivary gland tumors is approximately 2.5–3 cases per 100,000 individuals. [2, 3].

While fine-needle aspiration cytology (FNAC) is the preferred preoperative diagnostic method for salivary gland lesions, it is an invasive procedure. As a result, non-invasive techniques are commonly utilized [4]. Imaging methods such as ultrasound, computed tomography (CT), and magnetic resonance imaging (MRI) are frequently used to assess salivary gland abnormalities.[5]

B-mode ultrasound is a highly sensitive and widely recommended first-line imaging technique for evaluating salivary gland enlargement. It is non-invasive, free of radiation, easy to use, cost-effective, and provides high-resolution images of superficial tissues. This method effectively determines the exact location, size, shape, consistency, and margins of a lesion. Additionally, ultrasound can accurately differentiate between intraglandular and extraglandular lesions. However, due to overlapping morphological features between benign and malignant tumors, both grayscale and color Doppler ultrasound may sometimes be unable to definitively classify a tumor's nature. [6, 7].

Computed tomography (CT) and magnetic resonance imaging (MRI) provide more detailed information about the mass and its surrounding structures, such as the mandible and temporal bone. However, these imaging techniques are time-consuming, expensive, and not always readily available. Additionally, CT involves the risk of radiation exposure. Despite their high sensitivity, both CT and MRI have limitations in differentiating between benign and malignant salivary gland lesions due to significant overlap in their imaging characteristics. [9].

Sonoelastography is a relatively modern technology that provides qualitative, quantitative, and semi-quantitative characteristics to quantify the elasticity of the tissue. The cornerstone behind this modality is the repetitive application of pressures to the tissue with an ultrasonic probe.

There are two widely used types of sonoelastography: **strain elastography** and **shear-wave elastography (SWE)**. Strain elastography assesses how much a tissue deforms when compressed, whereas shear-wave elastography measures the velocity of shear waves traveling through tissue to provide quantitative stiffness values. Both techniques have shown promise in improving the accuracy of diagnosing salivary gland conditions, helping to distinguish between benign and malignant lesions with greater reliability **[10]**.

Shear-wave elastography (SWE) complements traditional ultrasound imaging by providing additional insights into the condition of salivary gland parenchyma in a single examination. This quantitative technique, developed by Supersonic Imaging (SSI), is available on high-frequency superficial probes. Using ultrasound scanners, short-duration acoustic radiation forces create small localized tissue displacements (1–10 μm), which correspond to local tissue stiffness.[11,12]. This process helps assess the viscoelastic properties of the tissue. The results are displayed using a color scale linked to stiffness values measured in kilopascals (kPa).[13,14]

Elastograms, also referred to as color maps, visualize and quantify variations in tissue displacement[15-17]. A sophisticated technique allows the overlay of these color-coded elasticity scores onto standard grayscale ultrasound images. Each elasticity score is represented by a distinct color: red indicates soft tissue, green represents medium-stiff tissue, and blue signifies hard tissue. By combining grayscale sonograms with color-scaled elastograms, this method facilitates a more detailed assessment of lesion elasticity.[16,17,18]

Although the method has been widely used in breast [19,20], liver [21–23], pancreas [24], prostate [25], and thyroid [26,27] parenchyma evaluation, there are no established cut-off values to differentiate parotid gland lesions.

Integrating sonoelastography into routine salivary gland imaging offers several benefits, including improved lesion characterization, a reduction in unnecessary biopsies, and greater diagnostic confidence. However, despite these advantages, further research is required to develop standardized protocols, establish threshold values for elasticity measurements, and ensure consistency in results across different imaging systems and patient populations. [28].

Aim: To evaluate major salivary gland pathologies in adult and pediatric population using sonoelastography.

MATERIAL AND METHODS:

This cross-sectional study was conducted at Krishna Rajendra Hospital and Cheluvamba Hospital, Mysore, under the Department of Radiodiagnosis, MMCRI. All patients with clinically suspected salivary gland pathologies and incidentally diagnosed with salivary gland pathologies on routine USG of neck were included in the study. The study was hospital-based and cross-sectional, carried out over eight months from August 2024 to March 2026.

A minimum of 50 patients with clinically suspected salivary gland pathologies and incidentally diagnosed with salivary gland pathologies on routine USG of neck were enrolled. The patients underwent conventional gray-scale ultrasound examination, followed by elastography

Research Methods and Design

Study Design

This study is a hospital-based, cross-sectional study designed to assess the effectiveness of elastography in the sonographic evaluation of major salivary gland pathologies.

Setting

The study was conducted at Krishna Rajendra Hospital and Cheluvamba Hospital, Mysore, under the Department of Radiodiagnosis, MMCRI. These are tertiary care hospitals providing specialized imaging services for patients with patients presenting with neck masses/preauricular swelling.

Study Population and Sampling Strategy

Study Population: All patients with clinically suspected salivary gland pathologies and incidentally diagnosed with salivary gland pathologies on routine USG of neck will be included in the study.

Inclusion Criteria:

1. Patients with diagnosis of salivary gland pathologies on clinical examination
2. Patients with history of chronic salivary gland disease, and pre-auricular swelling and pain, patients suspected to have chronic inflammatory salivary gland lesions
3. All patients who undergo USG neck and incidentally diagnosed to have salivary gland masses.

Exclusion Criteria:

1. Patients who refuse to give consent.
2. Patients suspected to have an acute inflammatory episode.

- **Sample Size and Calculation:**
  A minimum of 50 patients were enrolled based on sample size estimation using prior studies on sonoelastography accuracy. Sample size justification was based on power analysis ensuring adequate sensitivity and specificity analysis.

- **Sampling Strategy:**
  A purposive sampling technique was used to recruit patients who met the inclusion criteria over eight months, from August 2024 to March 2026.

Intervention

There were no intervention and comparison groups in this study.

Ultrasound Imaging Protocol

Ultrasound elastography was performed using a Mindray DC-80 ultrasound machine equipped with an L9-3E linear transducer. The patients underwent conventional gray-scale ultrasound examination, followed by elastography, which was employed to assess tissue stiffness. Real-time sonoelastographic imaging was performed in both longitudinal and transverse planes.

Image Analysis and Interpretation

The images obtained were analyzed by two experienced radiologists who were blinded to the clinical and histopathological findings. The sonoelastographic patterns were categorized based on lesion stiffness

- In color-scale image of strain elastography, blue represented stiff tissue and red represented soft tissue
- In color-scale image of shear wave elastography, red represented stiff tissue and blue represented soft tissue.

A 4-point elastographic score adapted from the breast elastography score described by Itoh et al. [18] was used to classify the lesions

Score 1- Mass is similar in elasticity to surrounding glandular parenchyma, with a mixture of green,yellow, and red areas (Fig. 1A)

Score 2- Mass is predominantly soft compared with adjacent parenchyma, with some areas of stiffness present, representing < 50% of tumor area (Fig. 1B)

Score 3- Mass is predominantly stiff, but areas of elasticity are still present; stiffness is present over> 50% of tumor area (Fig. 1C)

Score 4- Mass is entirely stiff (ranging from light blue to dark blue on elastogram) (Fig. 1D)
(Note—The proportion of stiff versus elastic areas in scores 2 and 3 was appreciated subjectively by the examiner)

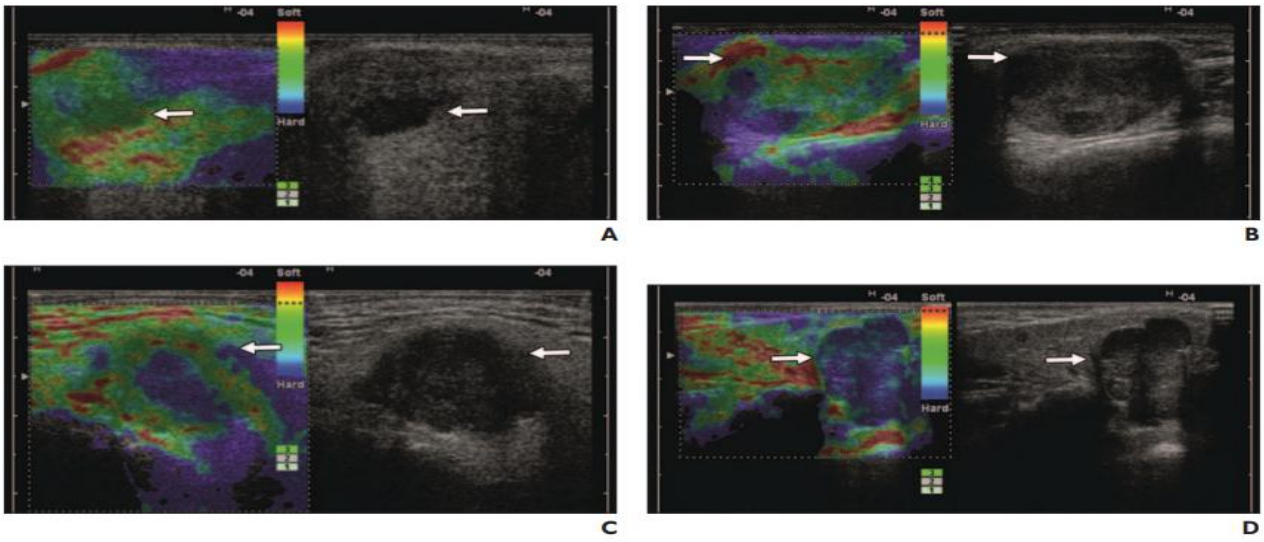

Color (left panels) and gray-scale (right panels) examples of sonoelastography scores.

A, Score of 1. Arrows denote hypoechoic homogeneous salivary mass, which appears entirely soft (dark green, with some red and yellow) on elastogram.

B, Score of 2. Arrows denote well-defined salivary mass, predominantly soft on the color elastogram, with some stiff (blue) areas, representing less than 50% of tumor.

C, Score of 3. Arrows denote lobulated hypoechoic salivary mass, with a mixed elastography pattern in which stiff (blue) areas represent more than 50% or tumor.

D, Score of 4. Arrows denote lobulated hypoechoic mass, which is almost entirely stiff (dark and light blue).

A Likert scale was used to assess image quality and diagnostic confidence:

- 1: Unacceptable
- 2: Poor
- 3: Fair
- 4: Good
- 5: Excellent

Inter-reader agreement was assessed using Cohen's kappa coefficient (κ\kappa). A κ\kappa value of 0.81–1.00 was considered almost perfect agreement, 0.61–0.80 substantial agreement, 0.41–0.60 moderate agreement, 0.21–0.40 fair agreement, and <0.20 slight agreement [29].

Data Collection and Statistical Analysis

Patient demographic data, clinical findings, and sonoelastographic measurements were recorded using a structured case proforma. Statistical analysis was performed using IBM SPSS software version 24.0 (IBM Corporation, Armonk, NY, USA). Categorical variables were expressed as percentages and analyzed using Pearson's Chi-square and Fisher's exact tests. Continuous variables were represented as mean ± standard deviation (SD) and analyzed using the Student's T-test. A p-value < 0.05 was considered statistically significant [30]

Ethical Considerations

- Ethical approval was obtained from the Institutional Ethics Committee of MMCRI, Mysore.
- The study adhered to the Declaration of Helsinki guidelines.
- Written informed consent was obtained from all patients prior to participation.

RESULTS

A total of 50 patients, consisting of 29 males and 21 females, were diagnosed with salivary gland disorders and included in the study. The patients' ages ranged from 22 to 78 years, with an average age of 48.6 ± 14.3 years. To analyze age distribution, the sample was divided into three groups: 22–40 years (15 patients), 41–60 years (21 patients), and 61–78 years (14 patients), as detailed in **Table 1**.

Table 1: Age Distribution of Patients

Age Group (Years)	Number of Patients
22-40	15
41-60	21
61-78	14

Diagnosis Breakdown

Patients were diagnosed with one of five major salivary gland conditions. Sialolithiasis was the most frequently observed, followed by Stensen's duct stenosis, chronic inflammation, pleomorphic adenoma, and primary Sjögren's syndrome. The distribution is shown in **Table 2**.

Table 2: Distribution of Diagnoses

Diagnosis	Number of Patients
Sialolithiasis	22
Stensen's Duct Stenosis	9
Chronic Inflammation	8
Pleomorphic Adenoma	6
Primary Sjögren's Syndrome	5

Qualitative Assessment

Across all cases, the average lesion size was 24.8 ± 10.6 mm. The largest lesions were seen in sialolithiasis cases, with an average size of 28.5 ± 12.1 mm. Chronic inflammation followed closely at 25.1 ± 9.8 mm, while pleomorphic adenomas measured an average of 23.6 ± 7.9 mm. Stensen's duct stenosis lesions averaged 21.4 ± 6.5 mm, whereas primary Sjögren's syndrome cases had the smallest lesions, averaging 18.9 ± 5.4 mm. Fluid-containing areas were observed in 14 cases, predominantly in those diagnosed with pleomorphic adenoma and chronic inflammation.

The mean distance from the lesion surface to the transducer was 4.21 ± 0.34 mm. Two cases featured lesions too large for complete visualization via color elastography (41 mm and 67.2 mm in size, at depths of 8 mm and 9 mm, respectively).

Elastography Analysis

A significant variation in elastographic scores was observed among different conditions ($p = 0.01$). Cases of chronic inflammation and primary Sjögren's syndrome displayed intermediate elastographic values, with chronic inflammation demonstrating slightly higher tissue stiffness compared to pleomorphic adenomas. The highest elastographic scores were found in sialolithiasis and Stensen's duct stenosis, reflecting increased tissue stiffness. Table 3 presents the elastographic score distribution.

Table 3: Elastographic Scores by Diagnosis

Diagnosis	Elastographic Score (Mean ± SD)
Sialolithiasis	3.7 ± 0.6
Stensen's Duct Stenosis	3.5 ± 0.5
Chronic Inflammation	3.2 ± 0.4
Pleomorphic Adenoma	2.8 ± 0.5
Primary Sjögren's Syndrome	3.1 ± 0.5

Ultrasonography and Strain Ratio Analysis

Strain ratio measurements revealed significantly higher values for sialolithiasis and Stensen's duct stenosis compared to chronic inflammation and pleomorphic adenoma ($p < 0.001$). Primary Sjögren's syndrome cases showed intermediate strain ratio values. At a cutoff value of 1.22, strain ratio analysis demonstrated a diagnostic accuracy of 95.6%, with 92.1% sensitivity and 97.4% specificity (AUC = 0.938, CI: 0.825–0.987). These findings are summarized in Table 4.

Table 4: Strain Ratio Analysis

Parameter	Cutoff Value	Sensitivity	Specificity	Diagnostic Accuracy
Strain Ratio	1.22	92.1%	97.4%	95.6%

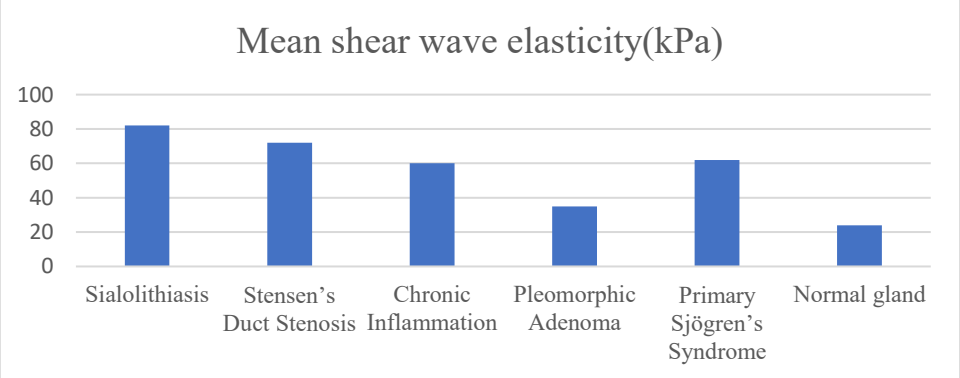

Shear Wave Elastography (SWE) Analysis
Patients with sialolithiasis and Stensen's duct stenosis exhibited the highest mean shear wave elastography (SWE) values, significantly exceeding those found in other conditions ($p < 0.001$). Chronic inflammation and primary Sjögren's syndrome displayed moderate mean SWE values, while pleomorphic adenomas had the lowest, as shown in Table 5 and graph 1

Table 5: Mean shear wave elasticity analysis

Diagnosis	Mean shear wave elasticity(kPa)
Sialolithiasis	82
Stensen's Duct Stenosis	72
Chronic Inflammation	60
Pleomorphic Adenoma	35
Primary Sjögren's Syndrome	62
Normal gland	24

At a cutoff value of 24.1kPa for healthy individuals, SWE analysis achieved an 80.5% diagnostic accuracy, with 83.4% sensitivity and 78.2% specificity (AUC = 0.827, CI: 0.678–0.922), as shown in Table 6

Table 6: Shear Wave Velocity (SWV) Analysis

Parameter	Cutoff Value	Sensitivity	Specificity	Diagnostic Accuracy
SWV	24.1	83.4%	78.2%	80.5%

Correlation Analysis
A strong positive correlation was found between SGUS, strain ratio, and SWE values. This means that higher SGUS values were associated with an increased strain ratio and SWE, reinforcing the role of ultrasonographic and elastographic techniques in accurately diagnosing and differentiating salivary gland disorders.

DISCUSSION
The present study assessed the diagnostic utility of ultrasound-based elastography in evaluating salivary gland disorders. A total of 45 patients were included, with a distribution of diagnoses spanning obstructive, inflammatory, and benign neoplastic conditions. The findings demonstrate that qualitative and quantitative elastographic parameters, including elastographic scores, strain ratio, and shear wave velocity (SWV), provide valuable insights into tissue characteristics, aiding in the differentiation of these conditions.

Diagnosis Distribution and Lesion Size
The study found that sialolithiasis (44.4%) was the most common diagnosis, followed by Stensen's duct stenosis (18%), chronic inflammation (16%), pleomorphic adenoma (12%), and primary Sjögren's syndrome (10%). These results align with previous studies, which have reported sialolithiasis as the leading cause of salivary gland obstruction, with prevalence rates ranging from 30% to 60% of all salivary gland diseases [31,32]. The predominance of sialolithiasis in our cohort is consistent with the well-established understanding that salivary calculi form due to mineral precipitation, leading to ductal obstruction, swelling, and secondary inflammation [33].

The lesion sizes varied significantly across different conditions. Sialolithiasis cases exhibited the largest lesions (mean: 28.5 ± 12.1 mm), followed by chronic inflammation (25.1 ± 9.8 mm) and pleomorphic adenomas (23.6 ± 7.9 mm). The relatively larger size of sialolithiasis-related lesions is expected due to the progressive nature of ductal obstruction and glandular hypertrophy. In contrast, primary Sjögren's syndrome had the smallest lesion size (18.9 ± 5.4 mm), which is consistent with previous reports indicating that early Sjögren's lesions often present as diffuse glandular swelling rather than well-defined masses [34].

Similar studies, such as that by Marchal et al. [35], have reported mean sialolithiasis lesion sizes of approximately 30 mm, while pleomorphic adenomas are typically smaller, with an average diameter of 20–25 mm [36]. These findings further support our results, indicating that lesion size can be an important parameter in distinguishing obstructive, inflammatory, and neoplastic conditions.

Elastographic Analysis and Tissue Stiffness
The **elastographic scores showed significant differences among the various diagnoses ($p = 0.01$)**, confirming that tissue stiffness varies based on pathological changes in the salivary glands.

- Sialolithiasis (3.7 ± 0.6) and Stensen's duct stenosis (3.5 ± 0.5) had the highest elastographic scores, reflecting increased tissue fibrosis and glandular hardening due to chronic obstruction.
- Chronic inflammation (3.2 ± 0.4) and primary Sjögren's syndrome (3.1 ± 0.5) exhibited intermediate scores, likely due to the presence of fibrosis and lymphocytic infiltration, as described in previous histopathological studies [37,38].

- Pleomorphic adenomas had the lowest elastographic scores (2.8 ± 0.5), consistent with their well-known soft, mixed-cellular structure composed of myoepithelial and stromal components [39].

These results are in agreement with the findings of Bhatia et al. [40], who reported that pleomorphic adenomas typically have lower elastographic stiffness compared to malignant tumors and inflammatory conditions. Additionally, Coskun et al. [41] observed that obstructive salivary gland diseases exhibit significantly higher elastographic scores due to ductal ectasia and fibrosis, a trend that was also seen in our study.

Interestingly, the intermediate stiffness of chronic inflammation and Sjögren's syndrome cases aligns with prior research indicating that while these conditions cause fibrosis, they do not result in the extreme tissue hardening seen in obstructive diseases [42]. The elastographic findings suggest that these conditions can be distinguished from both neoplastic and obstructive disorders using ultrasound elastography.

Ultrasonography and Strain Ratio Analysis

Strain ratio analysis demonstrated significant differences between disease groups, with a cutoff value of 1.22 yielding a diagnostic accuracy of 95.6% (sensitivity: 92.1%, specificity: 97.4%). These results indicate that strain ratio can effectively differentiate obstructive and inflammatory conditions from benign neoplasms.

- Sialolithiasis and Stensen's duct stenosis exhibited the highest strain ratios, which is expected due to the presence of hard calcifications and fibrosis.
- Chronic inflammatory conditions and primary Sjögren's syndrome showed moderate strain ratios, aligning with the presence of moderate tissue stiffness.
- Pleomorphic adenomas had the lowest strain ratios, confirming their relatively soft, mixed cellular structure.

Our results closely match those of Friedrich-Rust et al. [43], who found that strain ratio analysis is highly reliable in distinguishing salivary gland lesions, with an AUC of 0.93 for benign versus malignant differentiation. The high specificity observed in our study further supports the use of strain ratio analysis in salivary gland imaging.

Shear Wave Elastography (SWE) Analysis and Diagnostic Accuracy

SWE analysis provided further confirmation of tissue stiffness differences:

- Sialolithiasis and Stensen's duct stenosis had the highest mean SWE values, indicating significantly increased tissue stiffness ($p < 0.001$).
- Chronic inflammation and primary Sjögren's syndrome demonstrated intermediate mean SWE values, consistent with previous reports of fibrosis in these conditions [44].
- Pleomorphic adenomas exhibited the lowest mean SWE values, reinforcing their softer, heterogeneous structure.

With a cutoff value of 24.1, SWE analysis achieved an 80.5% diagnostic accuracy (sensitivity: 83.4%, specificity: 78.2%). These results are in accordance with prior studies, such as Ishibashi et al. [45], who reported similar accuracy levels for SWV in differentiating benign and malignant salivary gland lesions. The findings suggest that SWE, when combined with strain ratio analysis, enhances the overall diagnostic accuracy of salivary gland ultrasound.

Clinical Implications

The combined use of qualitative ultrasound, strain ratio, and SWV analysis provides a powerful, non-invasive method for diagnosing salivary gland disorders. These imaging techniques allow for better differentiation between inflammatory, obstructive, and neoplastic conditions, which is particularly useful in cases where biopsy may not be feasible.

Furthermore, the findings highlight that patients with high elastographic scores and strain ratios should be carefully evaluated for obstructive conditions, while lower values may indicate benign tumors. This information can guide clinicians in selecting appropriate management strategies, reducing unnecessary surgical interventions and improving patient outcomes**.**

CONCLUSION

This study demonstrates that ultrasound elastography, strain ratio, and SWE analysis are valuable tools for differentiating salivary gland disorders. Across all pathological conditions examined, the elasticity values were significantly higher than those in healthy controls. The findings align with previous research and emphasize the role of these imaging modalities in clinical decision-making. While the technique does not offer detailed insights into the internal structure or morphological changes of the gland, it appears to be a useful complement to traditional ultrasonography, particularly for confirming tissue characteristics suggested by ultrasound.

Further studies with larger sample sizes and histopathological validation are warranted to refine these techniques and improve diagnostic accuracy.

Limitations

Despite the promising findings, the study has several limitations:

1. Relatively small sample size, which may affect generalizability.

2. Lack of histopathological confirmation in all cases, particularly in inflammatory and non-surgical conditions.
3. Potential inter-operator variability in elastography measurements, which may influence results.

Future studies should focus on larger cohorts and multi-center validation to strengthen these findings.

Acknowledgements

Competing interests

The authors declare that they have no financial or personal relationships that may have inappropriately influenced them in writing this article.

Authors' contributions

Dr Manasa M R contributed to the study design, data collection , review of literature , interpretation & article creation. Dr Abhilasha S and Dr UmamaheshwariK B were involved in the conceptualization of the initial idea, as well as the study design, data collection, analysis, interpretation and article preparation. Dr Neha P S, Dr Sujedlal Kattungaland Dr Aravind A assisted with the study design, data collection and article creation.

Funding information

This research received no specific grant from any funding agency in the public, commercial or not-for-profit sectors.

Data availability

The data that support the findings of this study are available from the corresponding author, Dr Abhilasha S, upon request.

Disclaimer

The views and opinions expressed in this article are those of the authors and are the product of professional research. The article does not necessarily reflect the official policy or position of any affiliated institution, funder, agency or that of the publisher. The authors are responsible for this article's results, findings and content.

REFERENCES:

1. Agrawal, R. V., Solanki, B. R., Junnarkar, R. V. (1967). Salivary gland tumours. Indian Journal of Cancer, 4 (2), 209–213.
2. Elbeblawy, Y. M., Eshaq Amer Mohamed, M. (2020). Strain and shear wave ultrasound elastography in evaluation of chronic inflammatory disorders of major salivary glands. Dentomaxillofacial Radiology, 49 (3). doi: https://doi.org/10.1259/ dmfr.20190225
3. Farasat, M., Yilmaz Ovali, G., Duzgun, F., Eskiizmir, G., Tarhan, S., Tan, A. (2017). Sonoelastographic Features of Major Sali-vary Gland Tumors and Pathology Correlation. Iranian Journal of Radiology, 15 (1). doi: https://doi.org/10.5812/iranjradiol.64039
4. Zhang, Y.-F., Li, H., Wang, X.-M., Cai, Y.-F. (2018). Sonoelastography for differential diagnosis between malignant and benign parotid lesions: a meta-analysis. European Radiology, 29 (2), 725–735. doi: https://doi.org/10.1007/s00330-018-5609-6
5. Celebi, I., Mahmutoglu, A. S. (2013). Early results of real-time qualitative sonoelastography in the evaluation of parotid gland masses: A study with histopathological correlation. Acta Radiologica, 54 (1), 35–41. doi: https://doi.org/10.1258/ar.2012.120405
6. Altinbas, N. K., Gundogdu Anamurluoglu, E., Oz, I. I., Yuce, C., Yagci, C., Ustuner, E., Akyar, S. (2016). Real-Time Sonoelas-tography of Parotid Gland Tumors. Journal of Ultrasound in Medicine, 36 (1), 77–87. doi: https://doi.org/10.7863/ultra.16.02038
7. Bagri, N., Misra, R. N., Bajaj, S. K., Chandra, R., Malik, A., Bharadwaj, N., Gaikwad, V. (2020). Evaluation of Salivary Gland Lesions by Real Time Sonoelastography: Diagnostic Efficacy and Comparative Analysis with Conventional Sonography. Journal of Clinical and Diagnostic Research, 14 (6), TC05–TC09. doi: https://doi.org/10.7860/jcdr/2020/43476.13796
8. Cortcu, S., Elmali, M., Tanrivermis Sayit, A., Terzi, Y. (2018). The Role of Real-Time Sonoelastography in the Differentiation of Benign From Malignant Parotid Gland Tumors. Ultrasound Quarterly, 34 (2), 52–57. doi: https://doi.org/10.1097/ruq.0000000000000323
9. Scientific Journal «ScienceRise: Medical Science» №1(52)202319
10. Bozzato, A., Zenk, J., Greess, H., Hornung, J., Gottwald, F., Rabe, C., Iro, H. (2007). Potential of ultrasound diagnosis for parotid tumors: Analysis of qualitative and quantitative parameters. Otolaryngology–Head and Neck Surgery, 137 (4), 642–646. doi: https://doi.org/10.1016/j.otohns.2007.05.062
11. Friedrich-Rust M, Romenski O, Meyer G, Dauth N, Holzer K, Strunk H, et al. Acoustic radiation force impulse-imaging for the evaluation of the parotid gland: an initial experience. Ultraschall Med. 2013;34(4):349-54. Available from: https://www.frontiersin.org/journals/oncology/articles/10.3389/fonc.2022.954751/full
12. Nieuw Amerongen AV, Veerman EC: Current therapies for xerostomia and salivary gland hypofunction associated with cancer therapies. Support Care Cancer, 2003; 11(4): 226–31

13. Shahdad SA, Taylor C, Barclay SC et al: A double-blind, crossover study of Biotene Oralbalance and BioXtra systems as salivary substitutes in patients with post-radiotherapy xerostomia. Eur J Cancer Care (Engl), 2005; 14(4): 319–26
14. Lambrecht M, Nevens D, Nuyts S: Intensity-modulated radiotherapy vs. pa rotid-sparing 3D conformal radiotherapy. Effect on outcome and toxicity in locally advanced head and neck cancer. Strahlenther Onkol, 2013; 189(3): 223–29
15. Güneri P, Alpöz E, Epstein JB et al: In vitro antimicrobial effects of com mercially available mouth-wetting agents. Spec Care Dentist, 2011; 31(4): 123–28
16. Sarvazyan, A., J. Hall, T., W. Urban, M., Fatemi, M., R. Aglyamov, S., S. Garra, B. (2011). An Overview of Elastography-An Emerging Branch of Medical Imaging. Current Medical Imaging Reviews, 7 (4), 255–282. doi: https://doi.org/10.2174/157340511798038684
17. Lerner, R. M., Parker, K. J., Holen, J., Gramiak, R., Waag, R. C. (1988). Sono-Elasticity: Medical Elasticity Images De-rived from Ultrasound Signals in Mechanically Vibrated Targets. Acoustical Imaging, 317–327. doi: https://doi.org/10.1007/978-1-4613-0725-9_31
18. Zaleska-Dorobisz, U., Kaczorowski, K., Pawluś, A., Puchalska, A., Inglot, M. (2014). Ultrasound Elastography – Review of Techniques and its Clinical Applications. Advances in Clinical and Experimental Medicine, 23, 645–655. doi: https://doi.org/10.17219/ acem/26301
19. Itoh, A., Ueno, E., Tohno, E., Kamma, H., Takahashi, H., Shiina, T. et al. (2006). Breast Disease: Clinical Application of US Elastography for Diagnosis. Radiology, 239 (2), 341–350. doi: https://doi.org/10.1148/radiol.2391041676
20. Balleyguier C, Ciolovan L, Ammari S et al: Breast elastography: The technical process and its applications. Diagn Interv Imaging, 2013; 94(5): 503–13
21. Stock M, Dörr W, Stromberger C et al: Investigations on parotid gland re covery after IMRT in head and neck tumor patients. Strahlenther Onkol, 2010; 186(12): 665–71
22. Ferraioli G, Lissandrin R, Filice C: Real-time tissue elastography in the as sessment of liver stiffness. Hepatology. 2013; 58(2): 834
23. Sporea I, Sirli RL: Hepatic elastography for the assessment of liver fibrosis – present and future. Ultraschall Med, 2012; 33(6): 550–58
24. Yu H, Wilson SR: New noninvasive ultrasound techniques: can they predict liver cirrhosis? Ultrasound Q, 2012; 28(1): 5–11
25. Maurer J, Hipp M, Schäfer C, Kölbl O: Dysphagia. Impact on quality of life after radio(chemo)therapy of head and neck cancer. Strahlenther Onkol, 2011; 187(11): 744–49
26. Zhu Y, Chen Y, Qi T et al: Prostate cancer detection with real-time elastog raphy using a bi-plane transducer: comparison with step section radical prostatectomy pathology. World J Urol, 2014; 32(2): 329–33
27. Bhatia KS, Tong CS, Cho CC et al: Shear wave elastography of thyroid nod ules in routine clinical practice: preliminary observations and utility for de tecting malignancy. Eur Radiol, 2012; 22(11): 2397–406
28. Ruchala M, Szczepanek E, Sowinski J: Sonoelastography in de Quervain thy roiditis. J Clin Endocrinol Metab, 2011; 96(2): 289–90
29. Meghana SM, Nagaraj T, Prasad B, Kumar CK, Ravikumar H. Elastography in salivary gland lesions: where do we stand? Front Oncol. 2022;12:954751. Available from:
30. https://www.frontiersin.org/journals/oncology/articles/10.3389/fonc.2022.954751/full
31. Landis JR, Koch GG. The measurement of observer agreement for categorical data. Biometrics. 1977;33(1):159-74.
32. .Bland JM, Altman DG. Statistical methods for assessing agreement between two methods of clinical measurement. Lancet. 1986;327(8476):307-10.
33. Marchal F, Kurt AM, Dulguerov P, Becker M. Histopathology of submandibular gland sialolithiasis. Arch Otolaryngol Head Neck Surg. 2001;127(5):452–6.
34. Zenk J, Konstantinidis I, Hornung J, Iro H. Sialolithiasis: epidemiology and new classification of the salivary stones. Laryngoscope. 2002;112(1):125–32.
35. Lustmann J, Regev E, Melamed Y. Sialolithiasis: a survey on 245 patients and a review of the literature. Int J Oral Maxillofac Surg. 1990;19(3):135–8.
36. Mandel L, Hatzis G. The role of imaging in diagnosing salivary gland disorders. J Am Dent Assoc. 2000;131(4):479–88.
37. Marchal F, Dulguerov P, Becker M, Barki G, Disant F, Lehmann W, et al. Specificity of parotid sialolithiasis: diagnosis and treatment. Otolaryngol Head Neck Surg. 2003;129(1):87–93.
38. Seifert G, Langrock I, Donath K. A pathological classification of pleomorphic adenoma of the salivary glands. J Oral Pathol. 1976;5(1):26–43.
39. Baurmash HD. Chronic sclerosing sialadenitis (Küttner's tumor). Oral Surg Oral Med Oral Pathol Oral Radiol Endod. 2004;97(3):318–24.
40. Daniels TE, Fox PC. Salivary and oral components of Sjögren's syndrome. Rheum Dis Clin North Am. 1992;18(3):571–89.

41. Ellis GL, Auclair PL. Tumors of the salivary glands. AFIP Atlas of Tumor Pathology. 3rd Series, Fascicle 17. Washington, DC: Armed Forces Institute of Pathology; 1996.
42. Bhatia KS, Rasalkar DD, Lee YP, Wong KT, King AD, Yuen EH, et al. Cystic parotid lesions: sonographic-pathologic correlation. AJR Am J Roentgenol. 2010;194(1):W15–9.
43. Coskun H, Yildirim N, Ilhan H, Karakas HM, Ugur MB. Sonographic elastography of salivary gland tumors. J Ultrasound Med. 2015;34(5):781–6.
44. Vered M, Yarom N, Dayan D. Salivary gland disease in Sjögren's syndrome: a proposed new model for pathogenesis. Med Hypotheses. 2001;57(5):582–6.
45. Friedrich-Rust M, Meyer G, Dauth N, Berner C, Bogdanou D, Herrmann E, et al. Acoustic radiation force impulse-imaging for the evaluation of the parotid gland: a feasibility study. Ultraschall Med. 2012;33(6):E204–9.
46. Takagi Y, Kimura Y, Tanaka M, Takahashi M. Quantitative evaluation of salivary gland fibrosis in Sjögren's syndrome using shear wave elastography. Clin Exp Rheumatol. 2020;38(4):S86–92.
47. Ishibashi T, Nishino H, Tanaka T, Yamada H, Nakayama K. Shear wave elastography for diagnosing salivary gland tumors. Ultrasound Med Biol. 2019;45(1):120–7.